Underwater Video Image Restoration and Visual Communication Optimization Based on Improved Non Local Prior Algorithm

Tian Xia
School of Arts and Design, Qingdao University of Technology, Qingdao, 266033, China

***Abstract*—Underwater image processing should balance image clarity restoration and comprehensive display of underwater scenes, requiring image fusion and stitching techniques. The pixel level fusion method is based on pixels, and by fusing different image data, it eliminates stitching gaps and sudden changes in lighting intensity, preserves detailed information, and thus improves the accuracy of stitching images. In the process of restoring underwater video images without local priors, there is still room for optimization in steps such as removing atmospheric light values, estimating transmittance, and calculating dehazing images through regularization. Based on the characteristics of Jerlov water types, water quality is classified according to the properties of suspended solids, and each channel is adjusted to the compensation space to improve the restoration algorithm. Background light estimation is used to determine the degree of image degradation, select the optimal attenuation coefficient ratio, and restore the image. The experimental results show that it is crucial to choose a ratio of attenuation coefficients that is close to the actual water quality environment being photographed. Both this model and traditional algorithms have an accuracy rate of over 99.0%, with the accuracy of this model sometimes reaching 99.9%. Pixel level fusion and background light estimation technology optimize underwater images, improve stitching accuracy and clarity, enhance target detection and recognition, and have important value for marine exploration rigs.**

***Keywords*—Improving non local prior algorithms; underwater video images; visual communication effect; optical characteristic processing; image quality**

I. Introduction

A. Current Research Fields and Hotspots

In today's scientific field, underwater video image restoration and visual communication optimization have become hot research areas [1-2]. Due to the complex and variable optical characteristics in underwater environments, such as scattering and absorption phenomena in water bodies, the quality of underwater images is often very poor and filled with various noises and distortions [3-4]. This greatly limits the application and research of underwater images.

B. Issues and challenges

Underwater videos provide intuitive information about the underwater world, which is crucial for marine ecological research, underwater facility maintenance, and seabed resource exploration. However, harsh visual environments and unstable lighting conditions often lead to low quality underwater videos, affecting information extraction and analysis. Developing effective image restoration techniques to improve the quality of underwater videos is of great significance for expanding research on the understanding and utilization of the marine world. In response to these challenges, researchers are committed to finding more precise and efficient algorithms to improve the clarity and overall visual effects of underwater images, to better utilize these valuable underwater visual resources.

C. Gap with Previous Research

Although numerous studies are currently focused on underwater image restoration and visual effect optimization, these methods are often limited by the accuracy and efficiency of processing algorithms. The previous methods have not yet achieved complete satisfaction for researchers and practical applications in removing noise and distortion from underwater images, improving image contrast and clarity [5-6]. Therefore, there is an urgent need to further improve underwater image processing technology to enable observers to see underwater details more clearly.

D. The Necessity and purpose of research

This study proposes an underwater video image restoration and visual effect optimization method on the grounds of an improved non local prior (NLP) algorithm. It optimizes the processing flow to remove noise and distortion in underwater images. It enhances image contrast and clarity, allowing observers to see underwater details more clearly. This will further promote the development of underwater image processing technology and provide stronger support for related applications. It is expected that this research can play its due role in future scientific research and practical applications.

E. Research progress

The research will be conducted in five sections. Section I gives the introduction and Section II delves into related works. Section III is the research on underwater video image restoration and visual communication optimization on the grounds of improved NLP algorithms. Section IV is the experimental verification of the Section III. Section V is a summary of the research content and points out the shortcomings.

II. Related Works

Underwater video image processing has always been a key research area in the field of computer vision, as the

complexity and variability of underwater environments make image restoration a major challenge. Glassman et al. compared the effectiveness of three types of bait and two types of bait containers on bait free systems. The results indicate that BRUVS is effective in observing species richness in shallow and low visibility freshwater environments, but there is almost no evidence to suggest that the use of bait improves the effectiveness compared to non-bait RUVS [7]. Zhang et al. proposed an end-to-end dual generator model DuGAN on the grounds of generative adversarial networks for enhancing underwater images. Two discriminators are used to perform adversarial training on different regions of the image using different training strategies. This framework is easy to use, and both subjective and objective experiments have shown that it has achieved excellent results in the methods mentioned in the article [8]. Davies et al. conducted annual evaluations by comparing captured and uncaught populations inside and outside the MPA, as well as using bait based remote underwater video systems. The results indicate that comprehensive protection of the entire region with different benthic habitats is of great significance for the protection of fixed organisms that make significant contributions to fish habitats, as well as for maintaining sustainable fisheries and the interests of important protected species [9]. Zhu et al. proposed an image enhancement algorithm to improve the problem of image degradation caused by light absorption. The results indicate that the enhanced image has higher visibility, more details, and edge information [10]. Park et al. proposed a visibility enhancement technology for underwater cutting environments on the grounds of artificial neural networks to address the problem of deteriorating visibility in underwater construction environments. It uses two types of real image training on the grounds of GAN models, corresponding to cloudy input images. Experiments have shown that compared to traditional improvement techniques, trained neural networks can significantly improve the clarity of cloudy images [11].

NLP algorithms have been widely applied in image restoration, however, this algorithm still has some limitations for underwater video image restoration. Liang et al. proposed a color image restoration method that adaptively determines the size of dictionary atoms and discussed a model on the grounds of partial differential equation restoration methods. The results show that the algorithm can effectively overcome the shortcomings of fuzzy details and region expansion in fixed dictionary repair, and the repair effect is significantly improved [12]. Yang et al. proposed a modified DCP method that utilizes locally variable weighted 4-direction L-1 regularization and corresponding parallel algorithms to optimize transmission, further training deep neural networks, 4DL (1) R-net, to improve processing speed. The results have shown that this method is effective, can obtain clear details, maintain the natural clarity of the image, and significantly outperform the current state-of-the-art methods [13]. Wang et al. proposed a novel restoration algorithm that utilizes regional extremum and kernel optimization to address the issue of system blur in high-energy flash X-ray images. The results indicate that the algorithm can more accurately estimate the blur kernel, making the edges of the restored high-energy flash X-ray images clearer [14]. Lyu et al. proposed an ultrasound C-scan image restoration method that combines Richardson Lucy algorithm and defect measurement model to improve ultrasound image quality. The results show that the restoration method effectively improves the accuracy of ultrasound C-scan imaging, with a maximum error of only 10% and a minimum error of 2% for defect size [15]. Zhao et al. vectorized and grouped similar image segments, constructed a low rank noise matrix, and simultaneously processed the weighted minimization of all image segment groups through a new regularization term, accurately representing the sparsity and self-similarity of the image structure. The results show that the research method outperforms some existing optimization algorithms in both numerical and visual effects [16].

In summary, the widespread application of NLP algorithms in image restoration has laid the foundation for this field. However, facing the complex optical characteristics of underwater video images, existing algorithms have limited performance, and visual effect optimization also needs to be deepened. Faced with the complex optical characteristics of underwater video images, this study proposes a new underwater video image restoration and visual effect optimization scheme on the grounds of an improved NLP algorithm. It is expected that this improved method can more efficiently restore underwater images, enhance visual effects, and open up new possibilities for underwater video image research and application.

III. Underwater Video Image Restoration and Visual Communication Optimization Method on the Grounds of Improved NLP Algorithm

It elaborates on the implementation of underwater video image restoration on the grounds of NLPs, and explores the improvement strategy of underwater video image restoration on the grounds of this algorithm. It introduces the implementation strategy of underwater image fusion and stitching technology, and explores in depth how to improve visual communication effects through optimization strategies. It provides reference for underwater video image restoration and visual effect optimization, in order to promote the development of underwater vision research.

A. Implementation of Underwater Video Image Restoration on the Grounds of NLPs

Clustering in RGB color space (RGB) can approximate fogless images with hundreds of colors. The pixels of each cluster are derived from the entire image, non-local regions, forming a NLP [17]. This theory is on the grounds of an improved NLP algorithm for underwater video image restoration and visual effect optimization, which can achieve effective restoration of underwater video images. The flowchart of NLP restoration of images is shown in Fig. 1.

In Fig. 1, starting from an NLP, clustering is performed in a fog free image. Due to differences in depth and distance of field, there will be differences in transmittance. It clusters foggy images in RGB space, forming fog lines due to differences in transmittance. It uses clustering fog lines of foggy images to estimate transmittance, and then starts from the image degradation model to perform NL restoration of the

image. The estimation method of transmittance is different from the prior restoration of dark channels. Then it clusters the pixels of the foggy image into fog lines, estimates the initial transmittance $t(x)$, regularizes and refines the estimated transmittance, and finally performs image restoration. The image containing fog to be processed is shown in Eq. (1).

$$I_A(x) = I(x) - A \tag{1}$$

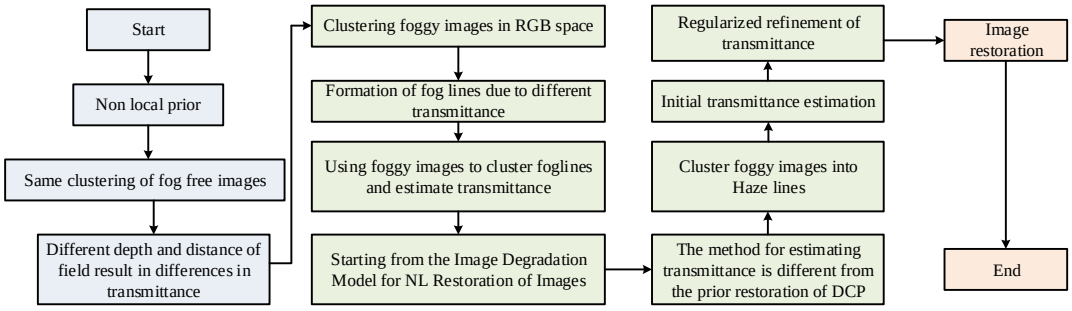

Fig. 1. Complex flowchart for NLP restoration of images.

In Eq. (1), $I(x)$ represents the image containing fog to be processed, and A represents the pre estimated atmospheric light value. A converts the RGB coordinate system of pixels in foggy images to point A as the coordinate origin [18-19]. The joint image degradation model is shown in Eq. (2).

$$I_A(x) = \left[r(x), \theta(x), \varphi(x) \right] \tag{2}$$

In Eq. (2), $r(x)$ is the distance from the origin A, $\theta(x)$ is longitude, and $\theta(x)$ is latitude. For each fog line in a foggy image, its two ends are a cluster of non-foggy image J and atmospheric light value A. The expression of transmittance with respect to the radius of the fog line is shown in Eq. (3).

$$r(x) = t(x) \times \left\| J(x) - A \right\|, 0 \le t(x) \le 1 \tag{3}$$

In Eq. (3), $t(x)$ is the transmittance and $r(x)$ is the radius of the fog line. The process of estimating transmittance from fog lines is shown in Fig. 2.

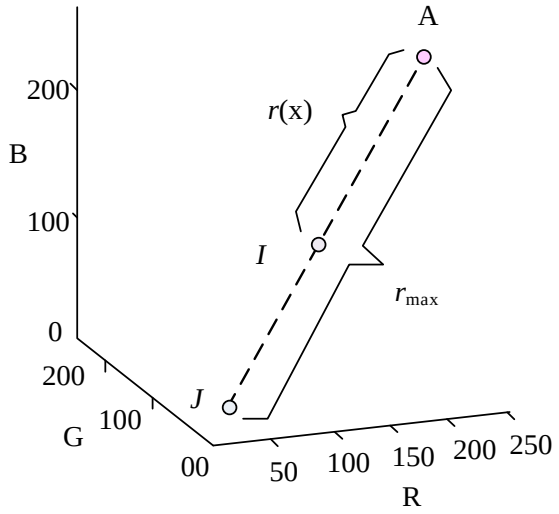

Fig. 2. The process of estimating transmittance from fog lines.

In Fig. 2, fog lines are formed by clustering foggy images to reveal differences in fog density. Then, the degradation model is used to initially estimate the transmittance, which directly affects the image clarity. It compares the estimated transmittance with the lower bound of transmittance, taking the larger one to ensure image authenticity, as real foggy images may not guarantee that each fog line contains fog free pixels. Finally, it smooths the transmittance map, suppresses noise, and enhances spatial continuity of the image. Its regularization refines the transmittance, as shown in Eq. (4).

$$\sum_x \frac{\left[\hat{t}(x) - \tilde{t}_{LB}(x) \right]^2}{\sigma^2(x)} + \lambda \sum_x \sum_{y \in N_x} \frac{\left[\hat{t}(x) - \tilde{t}(y) \right]^2}{\left\| I(x) - I(y) \right\|^2} \tag{4}$$

In Eq. (4), $\hat{t}(x)$ is the refined transmittance, N_x is the four neighborhoods centered on pixel N_x in the image, λ is the parameter used to balance the data and smoothing terms, and λ is the standard deviation of $\sigma^2(x)$. The restored image can be obtained from the degradation model, as shown in Eq. (5).

$$J(x) = \frac{\left\{ I(x) - \left[1 - \hat{t}(x) A \right] \right\}}{\hat{t}(x)} \tag{5}$$

B. Improvement of Underwater Video Image Restoration on the Grounds of NLP

The NLP underwater video image restoration process includes steps such as removing atmospheric light values, estimating transmittance, and calculating dehazing images through regularization. However, there is still room for optimization in improving the visibility of underwater images using this method, especially in transmittance estimation, where the R, G, and B channels are often uniformly processed [20]. This ignores the differences in underwater light wave attenuation and color distortion between channels. This study classifies water quality on the grounds of the characteristics of Jerlov water types and the properties of suspended solids, and adjusts each channel to the compensation space through the global attenuation coefficient ratio to improve the restoration algorithm. And it uses background light estimation to

determine the degree of image degradation, selects the optimal attenuation coefficient ratio, and restores the image. The transmittance is calculated and refined, as shown in Eq. (6) for different channels.

$$\begin{cases} A_R - I_R = e^{-\beta_R d} \cdot (A_R - J_R) \\ A_G - I_G = e^{-\beta_G d} \cdot (A_G - J_G) \\ A_B - I_B = e^{-\beta_B d} \cdot (A_B - J_B) \end{cases} \tag{6}$$

In Eq. (6), A is the background light and I is the type of water body. $e^{-\beta d}$ is the transmittance, $\beta(\lambda)$ is the attenuation coefficient, and $\beta(\lambda)$ is the depth of field. It performs power operations on the channel equations to obtain a moderate compensation space, as shown in Eq. (7).

$$\begin{bmatrix} (I_R(x) - A_R)^{\beta_{BR}} \\ (I_G(x) - A_G)^{\beta_{BG}} \\ (I_B(x) - A_B) \end{bmatrix} = t_B(x) \begin{bmatrix} (J_R(x) - A_R)^{\beta_{BR}} \\ (J_G(x) - A_G)^{\beta_{BG}} \\ (J_B(x) - A_B) \end{bmatrix} \tag{7}$$

In Eq. (7), β_{BR} is the blue red attenuation coefficient, and β_{BG} is the blue green attenuation coefficient. The smoothing factor is shown in Eq. (8).

$$\alpha(x) = \frac{D_M(I(x)) - \bar{D}_M - \sigma_M}{D_M^{\max} - \bar{D}_M} \tag{8}$$

In Eq. (8), $\alpha(x)$ is the smoothing factor, σ_M is the standard deviation, $D_M^{\max}$ is the maximum Mahalanobis distance, and $\bar{D}_M$ is the average Mahalanobis distance of the background light area. After estimating the transmittance, color attenuation compensation is performed to obtain the restored image. The scattering of light during its propagation in water can cause global color distortion. In order to make the image look like it is under white light, it can be corrected through white balance method after compensating for propagation loss. The implementation process of an improved underwater image restoration algorithm on the grounds of NLP prior is shown in Fig. 3.

In Fig. 3, edge detection is performed on the input image to determine the background light area and calculate the background light. On the grounds of the attenuation coefficient values under different water types, each channel is processed to estimate the initial transmittance. It performs soft cutout processing, uses enhanced images as guidance, and refines transmittance through filtering. It then restores the restored image and performs global white balance processing. Finally, its output refines the transmittance and restores the image.

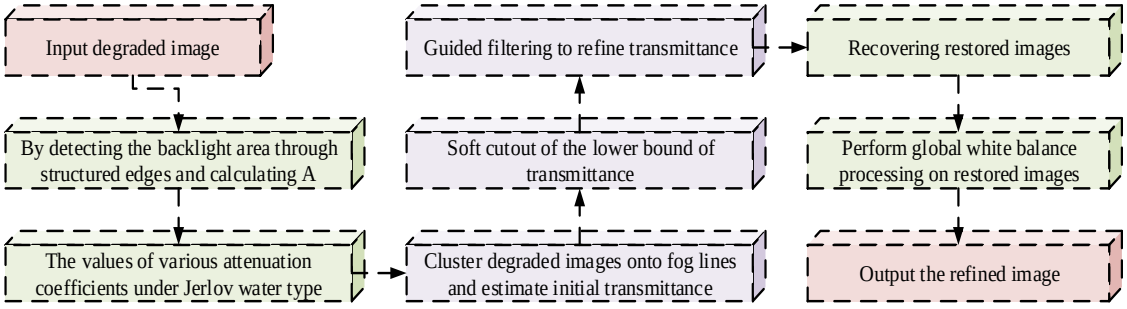

Fig. 3. Implementation of an improved underwater image restoration algorithm on the grounds of NLP prior.

C. Implementation Strategy for Underwater Image Fusion and Stitching Technology

In underwater image processing, in addition to clarity restoration, panoramic display of large-scale underwater scenes in complex environments is also required, which requires image fusion and stitching techniques. Image fusion is divided into pixel level, feature level, and decision level. Pixel level fusion has high accuracy but large data volume, feature level fusion reduces data volume but low accuracy, while decision level fusion has strong anti-interference ability, good real-time performance but low accuracy. In order to eliminate splicing gaps and sudden changes in lighting intensity, preserve detailed information and improve fusion accuracy, pixel level fusion is mainly used. Common methods include average value method, gradual in and out method, and multi band fusion method [21]. It takes the average of the pixel values of the corresponding points in two images within the overlapping area, and the average method is shown in Eq. (9).

$$I(x,y) = \begin{cases} I_1(x,y) & (x,y) \in R_1 \\ 0.5 \times [I_1(x,y) + I_1(x,y)] & (x,y) \in R_2 \\ I_2(x,y) & (x,y) \in R_3 \end{cases} \tag{9}$$

In Eq. (9), R_1 is the area that belongs only to the first image, R_2 is the area where the first and second images overlap, and R_2 is the area of the second image. The gradual in and out method assigns different weight values on the grounds of the distance between pixels and the overlapping boundary when processing regions of two overlapping images. Through this weighting method, the calculation of new pixel values can achieve a visual effect of smooth transition from one image to another. The pixel values corresponding to the fusion are shown in Eq. (10).

$$I(x,y)=\begin{cases} I_1(x,y) & (x,y)\in R_1 \\ d\times I_1(x,y)+(1-d)I_2(x,y) & (x,y)\in R_2 \\ I_2(x,y) & (x,y)\in R_3 \end{cases} \quad (10)$$

In Eq. (10), the meanings of R_1, R_2, and R_2 are the same as the average method. d is the gradient weight factor, and the image frames that are gradually approaching the middle are combined into the concatenated image. For a certain number of frame sets, a certain intermediate frame in the image set is selected as the initial reference image, and the image frames to be concatenated are selected from left to right in sequence. The image frame to concatenated image synthesis method on the grounds of intermediate frames is shown in Fig. 4.

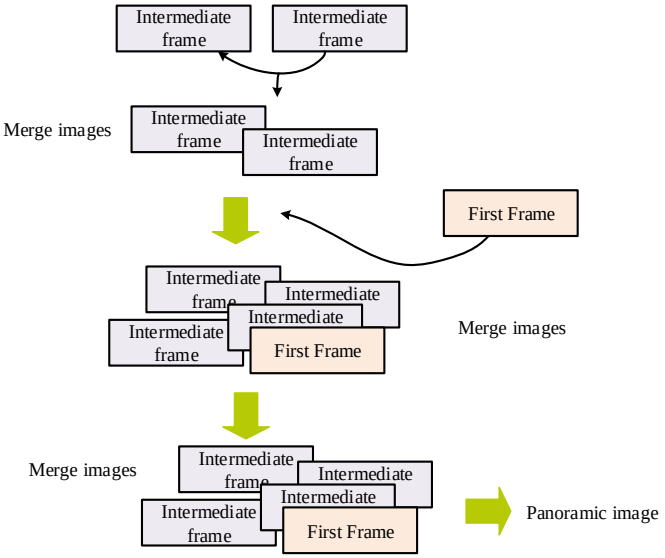

Fig. 4. Implementation of an improved underwater image restoration algorithm on the grounds of NLP prior.

In Fig. 4, it selects a frame in the middle as the initial reference image, registers it with the front and back frames through a projection transformation matrix, and fuses it using the gradual in and out method. It uses the fused image as a new reference image and sequentially selects the image to be stitched forward and backward for fusion. The advantage of this strategy is that it avoids the accumulation of transformation errors that may arise from frame by frame fusion. By using intermediate frames as the initial reference image, it can effectively consider the distance between all frames and the reference image, improve the overlap rate, and thus obtain a restored underwater panoramic image.

D. Optimization Strategies for Visual Communication Effects

The underwater image fusion and stitching technology optimizes visual effects, requiring comprehensive adjustments to image color, clarity, brightness, etc. Information graphical interaction technology also helps optimize visual effects, including two major elements: basic and interactive. The foundation ensures the accurate expression of information, provides a natural and convenient way for interaction, guides users to navigate, browse, filter, input, prompt and feedback, view conversion, etc. Macro to micro techniques handle complex graphics, allowing users to zoom in, scroll, jump, and move in the macro interface, observe details, and return to the macro interface to see the marked micro areas. Dynamic and interactive information prompts display hierarchical data information with organized structure, allowing users to see secondary information when browsing to a specified location. The comprehensive use of these technologies and strategies helps to improve underwater video image restoration and visual communication optimization methods on the grounds of NLP algorithms. In the underwater video image restoration and visual communication optimization method on the grounds of improved NLP algorithms, as shown in Fig. 5, interactive information prompt technology is an important strategy.

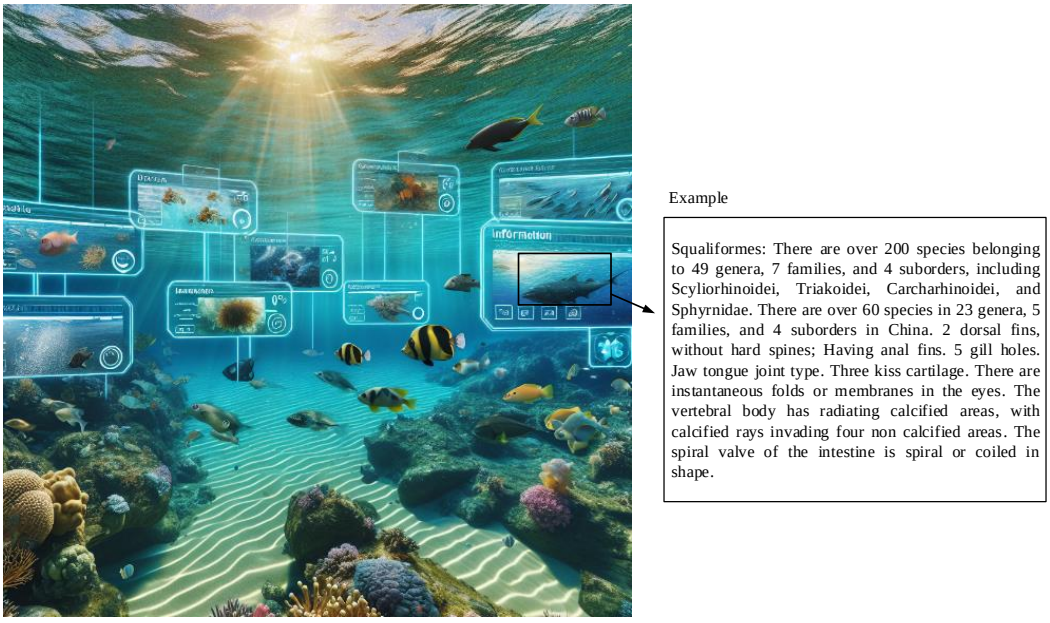

Fig. 5. Example of interactive information prompt technology.

This technology enables users to obtain relevant information by pointing to specific image elements, eliminating redundant operations. For underwater video images containing a large amount of information, interactive information prompt technology can provide dynamic display and concealment functions, and the content can change in real-time according to user operations. The dynamic prompt window provides users with real-time image information, improving the accessibility and usability of the information.

In the process of image restoration, dynamic query technology is the key to optimizing visual communication effects. It meets the needs of users for precise queries in a large amount of information. By using standard operating controls such as sliders, checkboxes, etc., users can define the display range of image information. For example, in video playback software, users can search for video information from a specific era on the grounds of the time of video release. The front-end logic of dynamic queries is clear, and the dominant power lies in the hands of users, ensuring efficient real-time interactive feedback. On the backend, the dynamic query engine processes user query requests, assembles query conditions, executes query instructions, parses parameters, searches for configurations, and determines query types. Finally, the search result data is objectified and formatted as a list of information that can be received by the control, which retrieves and renders the data, and returns it to the user interface. This achieves the precise query needs of users and improves the efficiency of information exploration. Fig. 6 shows interactive information prompts and dynamic query techniques. This combined application with interactive information prompt technology optimizes underwater video image restoration and visual communication effects on the grounds of NLP algorithms.

Fig. 6. Interactive information prompts and dynamic query techniques for optimizing visual communication effects.

IV. Analysis of Underwater Video Image Restoration and Visual Communication Optimization on the Grounds of Improved NLP Algorithm

Improving NLP algorithms can reduce noise and blur during image restoration and improve image quality. By combining interactive information prompts and dynamic query technology, the accessibility and usability of information can be enhanced, allowing users to accurately query a large amount of information, achieve efficient real-time interactive feedback, and improve information exploration efficiency.

A. Application Effect Analysis of Improved NLP Algorithm in Underwater Video Image Restoration

Improving the application effect of NLP algorithms is an important research direction in underwater video image restoration. This algorithm processes the local and non-local characteristics of the image, and the parameter settings of the model are shown in Table I. In the optimization analysis of visual communication effects, Sea rogman was selected to demonstrate the intermediate results of NL image restoration processing for underwater images. In this process, the parameter is set to 0.1. Table II shows the comparison results of the average gradient and information entropy after non local and dark channel prior restoration.

The improved NLP algorithm for restoring underwater video images can be observed through the SSIM index. For high-quality video frames such as Sea oral and Sea fish, this algorithm recovers SSIM values that surpass the Fast DCP algorithm. However, for low-quality video frames such as Underwater1_10, Underwater2_10, and Underwater2_340, their restored SSIM values are slightly lower. For specific effects, such as using Underwater1_10 as an example, it is necessary to refer to Fig. 7.

TABLE I. SYSTEM PARAMETER

Parameter Name	Description	Setting Value	Remarks
Operating System	Environment for running the software	Windows 10	64-bit
Processor	Hardware for executing the algorithm	Intel Core i7	2.6GHz
Memory	Temporary storage for algorithm and data	16GB	DDR4
Graphics Card	Hardware for processing images	NVIDIA GeForce GTX 1050	4GB
Algorithm Version	Executing algorithm	Improved Non-local Prior Algorithm	Latest version
Experiment Video	Testing data	Underwater video	1080p, 30fps
Experiment Environment	Place where the experiment is conducted	Laboratory	Temperature 25℃, Humidity 60%

TABLE II. COMPARISON OF AVERAGE GRADIENT AND INFORMATION ENTROPY AFTER NL AND DARK CHANNEL PRIOR RESTORATION

-	-	Original drawing				Information entropy E			
Image	Algorithm	R	G	B	Mean value	R	G	B	Mean value
Sea-coral	Original drawing	3.37	3.37	3.47	3.29	6.7	6.76	6.51	6.66
	Fast DCP	7.12	6.99	6.83	6.98	7.25	7.43	7.29	7.32
	NL	7.71	7.62	7.38	7.57	7.39	7.5	7.39	7.43
Sea-fish	Original drawing	0.5	0.48	0.49	0.49	4.98	6.03	5.63	5.55
	Fast DCP	1.18	1.09	1.14	1.14	4.8	6.65	6.09	5.85
	NL	1.88	1.38	1.92	1.73	6.36	7.22	7.18	6.92
Underwaterl_10	Original drawing	0.56	0.56	0.54	0.55	4.75	6.97	7.21	6.31
	Fast DCP	0.75	0.74	0.75	0.75	4.02	7.4	7.55	6.32
	NL	1.19	1.23	1.2	1.21	5.24	7.58	7.59	6.8
Underwater2_10	Original drawing	1.71	1.15	1.13	1.16	5.92	6.92	7.24	6.69
	Fast DCP	1.59	1.49	1.55	1.54	5.03	6.83	7.48	6.45
	NL	2.4	2.35	2.39	2.38	5.97	6.81	7.82	6.87
Underwater2340	Original drawing	0.62	0.58	0.55	0.58	5.16	7.01	6.97	6.38
	Fast DCP	0.79	0.75	0.78	0.77	5.24	7.06	7.27	6.15
	NL	1.18	1.14	1.34	1.25	4.25	7.24	7.67	6.84

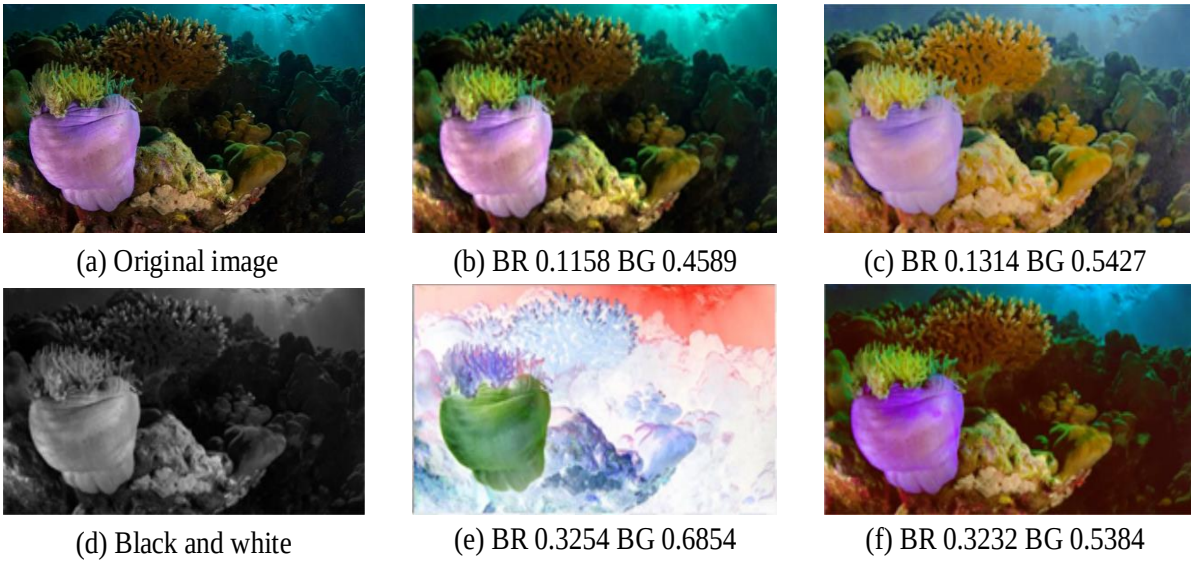

(a) Original image (b) BR 0.1158 BG 0.4589 (c) BR 0.1314 BG 0.5427

(d) Black and white (e) BR 0.3254 BG 0.6854 (f) BR 0.3232 BG 0.5384

Fig. 7. Image underwater1_10 results under different attenuation coefficient ratios.

In Fig. 7, the lower left grayscale image (d) shows the detected background light area, while Fig. 7(b), (c), (e), and (f) show the restored images obtained under different attenuation coefficient ratios. The attenuation coefficient ratio plays a crucial role in the process of image restoration. Using inaccurate ratios can lead to errors in the transmittance chart, resulting in color deviation in the reconstructed image. Therefore, it is crucial to choose a ratio of attenuation coefficients that is close to the actual water quality environment being photographed. The right choice can improve the restoration effect, while the wrong choice can lead to poor restoration effect.

B. Optimization Analysis of Visual Communication Effects

In the waters near the boundary island of Sanya, China, underwater videos were captured using the "Ocean Elf" sightseeing submarine. The experiment was conducted in the sea at a depth of 20-30 meters, with a submarine diving depth of 10-15 meters and visibility of 4-10 meters. The video was recorded using the iPhone 11 Pro rear camera. For detailed information on the video, please refer to Table III.

TABLE III. OPTIMIZATION ANALYSIS

Video file name	Duration (s)	Frame rate	Frame Image Size	Total Frames	Real keyframe rate
underwater1	6.0000	29.5357	544×980	232	8.0000
underwater2	8.0000	29.5357	980×544	247	9.0000
underwater3	10.0000	29.5357	640×480	296	10.0000
underwater4	12.0000	29.5357	1280×720	355	11.0000
underwater5	14.0000	29.5357	1920×1080	414	12.0000

To verify the superiority and accuracy of the model, experiments were conducted in underwater videos near the boundary island of Sanya, China. The sightseeing submarine takes photos in the sea area at a depth of 20-30 meters, with a diving depth of 10-15 meters and visibility of 4-10 meters. The experiment mainly used Underwater1 with a resolution of 544 * 960 and Underwater2 with a resolution of 980 * 544. The experiment first uses an improved keyframe extraction algorithm to obtain image frames, and then uses an improved algorithm for non-local underwater image restoration to process keyframes. After image registration and fusion, the matching results and fusion effects are displayed. For Underwater1 with poor image quality, the threshold T for new cluster partitioning is set to 18, and for good quality, it is set to 25. The experimental results are shown in Fig. 8.

In Fig. 8, the accuracy statistics of the model and traditional image restoration algorithms in 60 experiments are shown. Both the model and traditional algorithms have an accuracy rate of over 99.0%, and sometimes the accuracy of the model can even reach 99.9%, while the traditional model can only reach a maximum of 99.3%. In order to study the accuracy of the model in processing different underwater environments, 20 underwater videos were selected and 180 image data samples were collected for simulation of common underwater environments. The results are shown in Fig. 9.

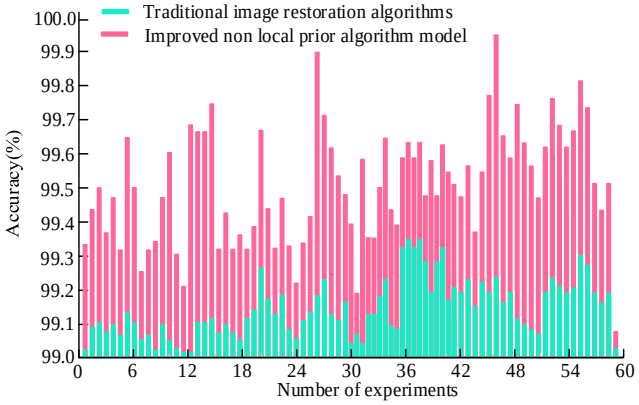

Fig. 8. Accuracy comparison chart.

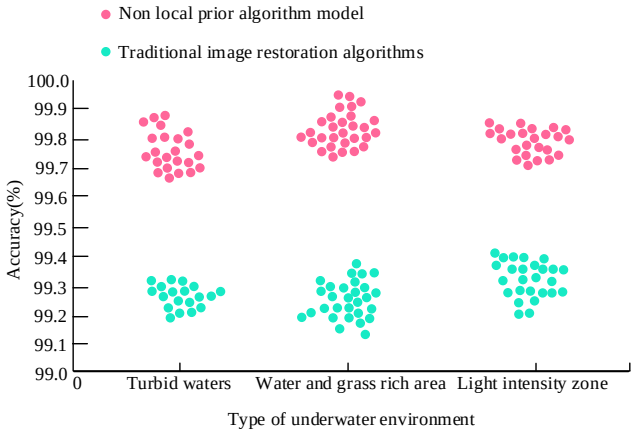

Fig. 9. Non-local prior model's accuracy in different underwater environments.

In Fig. 9, three types of seabed environments are covered: turbid waters, areas with abundant aquatic plants, and areas with strong sunlight. Regardless of the type of environment, the processing accuracy of NLP models exceeds 99.0%. The average accuracy of treating turbid water bodies is around 99.6%. This indicates that NLP models exhibit extremely high accuracy in restoring images of turbid water bodies. The average processing accuracy for areas with abundant water and grass is around 99.4%. This means that NLP models can effectively distinguish images in water grass rich areas and perform effective restoration processing, with an average accuracy of about 99.15% for areas with strong lighting.

V. CONCLUSION

Faced with the complexity of underwater environments and harsh lighting conditions, underwater image processing requires both restoration of image clarity and comprehensive display of underwater scenes, thus requiring the use of image fusion and stitching techniques. In this context, the research aims to optimize the NLP underwater video image restoration process and improve the accuracy of image processing. It classifies water quality on the grounds of Jerlov's water type characteristics, adjusts channel optimization restoration algorithms, and uses background light estimation to determine the degree of degradation. The results show that the attenuation coefficient ratio plays a crucial role in the image restoration process. The accuracy of this model can sometimes

even reach 99.9%, while traditional models only have a maximum of 99.3%. Not only that, NLP models can also effectively distinguish images in areas with abundant water and grass, and perform effective restoration processing. The average accuracy of processing in areas with strong lighting is about 99.15%. This study provides an effective method for improving the accuracy of underwater image processing. However, there are still shortcomings, such as the need to improve the accuracy of processing images in areas with strong lighting. Future research aims to further optimize the model, improve the accuracy of image processing for various complex underwater environments, and explore more image processing algorithms suitable for various complex underwater environments. This is to present the underwater scene more comprehensively while ensuring image clarity.

REFERENCES

[1] Chen Q, Zhang Z, Li G. Underwater image enhancement based on color balance and multi-scale fusion. IEEE Photonics Journal, 2022, 14(6): 1-10.

[2] Mathur M, Goel N. Enhancement of nonuniformly illuminated underwater images. International Journal of Pattern Recognition and Artificial Intelligence, 2021, 35(3): 1-23.

[3] Wei Y, Zeng A, Zhang X, Huang H. "RAG-Net: ResNet-50 attention gate network for accurate iris segmentation." IET Image Processing, 2022, 16(11): 3057-3066.

[4] Hu JW, Xie YT, Li SB, Du XY, Xiong NN. "An Edge Intelligence-based Generative Data Augmentation System for IoT Image Recognition Tasks." Journal of Internet Technology, 2021, 22(4): 765-778.

[5] Liao Y, Ragai I, Huang Z, Kerner S. "Manufacturing process monitoring using time-frequency representation and transfer learning of deep neural networks." Journal of Manufacturing Processes, 2021, 68(8): 231-248.

[6] Fu Z, Zheng L, Li J, Chen G, Yu T, Deng T. "DMvLNet: deep multiview learning network for blindly assessing image quality." Journal of Electronic Imaging, 2022, 31(5): 1-13.

[7] Glassman D M, Chhor A, Vermaire J C, Bennett J R, Cooke S J. Does bait type and bait container configuration influence the performance of remote underwater video systems in temperate freshwater lakes for assessing fish community structure? Hydrobiologia, 2022, 849(9): 1981-1994.

[8] Zhang H, Sun L, Wu L, Gu K. DuGAN: An effective framework for underwater image enhancement. IET Image Processing, 2021, 15(9): 2010-2019.

[9] Davies B F R, Holmes L, Rees A, Attrill M J, Cartwright A Y, Sheehan E V. Ecosystem Approach to Fisheries Management works—How switching from mobile to static fishing gear improves populations of fished and non-fished species inside a marine-protected area. Journal of Applied Ecology, 2021, 58(11): 2463-2478.

[10] Zhu D, Liu Z, Zhang Y. Underwater image enhancement based on colour correction and fusion. IET Image Processing, 2021, 15(11): 2591-2603.

[11] Park S K, Oh S Y, Shin J S, Park H, Kovalev V. A preliminary study on visibility improvement of turbid underwater images for dismantling of nuclear facilities. Annals of Nuclear Energy, 2021, 156(6): 1-8.

[12] Zhang L, Chang M, Chen R. Image inpainting based on sparse representation using self-similar joint sparse coding. Multimedia Tools and Applications, 2023, 82(13): 20215-20231.

[13] Yang Y, Long W, Li Y, Shi X, Gao L. Image defogging based on amended dark channel prior and 4-directional L1 regularisation.IET Image Processing, 2021, 15(11): 2454-2477.

[14] Wang X, Li Q, Xu J. High energy flash X-ray image restoration using region extrema and kernel optimization.IET Image Processing, 2021, 15(12): 2970-2985.

[15] Lyu D, Tian J, Hu H, He X. Ultrasonic C-scan image restoration method using the Richardson-Lucy algorithm and a flaw measurement model. Applied acoustics, 2022, 200(11): 1-9.

[16] Zhai L. Image restoration algorithm based on multiscale weighted Schatten p-norm minimization. Journal of Electronic Imaging, 2022, 31(2): 1-15.

[17] Omara A N, Salem T M, Elsanadily S, Elsherbini M M. SSIM-based sparse image restoration. Journal of King Saud University-Computer and Information Sciences, 2022, 34(8): 6243-6254.

[18] Sivaanpu A, Thanikaslam K. Scene-Specific Dark Channel Prior for Single Image Fog Removal. The International Journal on Advances in ICT for Emerging Regions, 2021, 14(3): 1-12.

[19] Cui Y, Zhi S, Liu W, Deng J, Ren J. An improved dark channel defogging algorithm based on the HSI colour space. IET Image Processing, 2022, 16(3): 823-838.

[20] Sabir A, Khurshid K, Salman A. Segmentation-based image defogging using modified dark channel prior. EURASIP Journal on Image and Video Processing, 2020, 2020(1): 1-14.

[21] Dornelas R S, Lima D A. Correlation Filters in Machine Learning Algorithms to Select De-mographic and Individual Features for Autism Spectrum Disorder Diagnosis. Journal of Data Science and Intelligent Systems, 2023, 3(1): 7-9.